Lilley, Eds. (Springer-Verlag, Berlin, 1989), vol. 1, pp. 186–195, and S. Leirmo and M. T. Record, Jr., in *ibid.*, vol. 4, pp. 123–151.
3. J.-H. Roe, R. R. Burgess, M. T. Record, Jr., *J. Mol. Biol.* **176**, 495 (1984); *ibid.* **184**, 444 (1985); H. Buc and W. R. McClure, *Biochemistry* **24**, 2712 (1985); J.-H. Roe and M. T. Record, Jr., *ibid.*, p. 4721.
4. U. Siebenlist, R. B. Simpson, W. Gilbert, *Cell* **20**, 269 (1980).
5. A. Spassky, K. Kirkegaard, H. Buc, *Biochemistry* **24**, 2723 (1985).
6. S. Sasse-Dwight and J. D. Gralla, *Proc. Natl. Acad. Sci. U.S.A.* **85**, 8934 (1988); D. W. Cowing, J. Mecsas, M. T. Record, Jr., C. A. Gross, *J. Mol. Biol.* **210**, 521 (1989).
7. H. Hayatsu and T. Ukita, *Biochem. Biophys. Res. Commun.* **29**, 556 (1967); J. A. Borowiec, L. Zhang, S. Sasse-Dwight, J. D. Gralla, *J. Mol. Biol.* **196**, 101 (1987).
8. S. Sasse-Dwight and J. D. Gralla, *J. Biol. Chem.* **264**, 8074 (1989).
9. T. V. O'Halloran, B. Frantz, M. K. Shin, D. M. Ralston, J. G. Wright, *Cell* **56**, 119 (1989).
10. J. T. Newlands, W. Ross, K. K. Gosink, R. L. Gourse, *J. Mol. Biol.* **220**, 569 (1991); M. Kainz and J. Roberts, *Science* **255**, 838 (1992); W. Wang, M. Carey, J. D. Gralla, *ibid.*, p. 450.
A synthetic λP_R fragment (−60 to +20 with respect to the transcription start site) was cloned into the Hpa I–Sal I sites of pBend5 (*22*), and the fragment containing the Eco RI–Hind III promoter was then cloned into pBluescript II SK (Stratagene) to generate plasmid pBR81. The λP_R-RNAP complexes were preformed for 15 min at the temperatures indicated (Fig. 1) with or without 10 mM $MgCl_2$ in 40-μl reactions containing 1 pmol of pBR81 DNA in 10 mM K Hepes (pH 7.5), 50 mM NaCl, 0.1 mM EDTA, 1 mM dithiothreitol, bovine serum albumin (100 μg/ml), and 87 nM RNA polymerase (*1*). $KMnO_4$ was added to a final concentration of 10 mM and incubated for 2 min, and the reactions were quenched with 10 μl of 3.5 M β-mercaptoethanol and 1.4 M sodium acetate. The samples were divided for probing modifications on each strand, 0.1 μg of λP_R plasmid DNA linearized with either Xba I at −68 or Sal I at +26 was added to generate a reference band for quantitative comparison, and the samples were phenolchloroform-extracted and precipitated with ethanol. DNA was then denatured with 0.2 M NaOH, neutralized, and precipitated with ethanol. A 17-residue primer [5.4 pmol of 5′-AATACGACTCACTATAG-3′ (for the top strand)] or 5′-TCGAGGGATCCTCTAGA-3′ (for the bottom strand) was annealed in 40 mM tris HCl (pH 7.5), 20 mM $MgCl_2$, and 50 mM NaCl at 65°C for 2 min with slow cooling to room temperature. The first three G residues of each primer-extension product were labeled by incubation for 5 min at 37°C with 1 U of Bst DNA Polymerase I (Bio-Rad) (*23*), 10 μCi of [α-^{32}P]deoxyguanosine triphosphate (dGTP), and either 0.6 μM deoxycytidine triphosphate (dCTP) or thymidine triphosphate (TTP). Deoxyadenosine triphosphate, dCTP, dGTP, and TTP (100 μM each) were added, and the reactions were incubated for 10 min at 65°C, then brought to a final concentration of 20 mM EDTA and 2 M ammonium acetate, precipitated with ethanol, washed with 70% ethanol, dried, counted (Cerenkov), and resuspended in 80% formamide, 10 mM NaOH, 0.1% xylene cyanol (Sigma), and 0.1% bromophenol blue. The samples were heated at 85°C for 3 min, and equivalent counts per minute from each were electrophoresed on an 8% acrylamide and 8 M urea sequencing gel in 0.5× TBE (45 mM tris HCl, 45 mM borate, 1 mM EDTA). The ratios of $KMnO_4$ reactivities in the presence and absence of Mg^{2+} at individual positions in the open region of the promoter are directly proportional to the relative extents of opening-accessibility of these positions if the intrinsic rate constant and the local [MnO_4^-] are unaffected by the addition of 10 mM Mg^{2+}. Mg^{2+} may increase the local concentration of MnO_4^- near the surface of the DNA polyanion and therefore account for part or all of the modest increases in $KMnO_4$ reactivity at many positions in the core of the open region. Such an effect cannot also explain the larger increases in reactivity at the boundaries of the open region. In addition, the observation that the $KMnO_4$ reactivity of −10T is approximately the same in the presence and absence of Mg^{2+} suggests that both the intrinsic rate constant and local [MnO_4^-] are unaffected by Mg^{2+}.
13. U. Siebenlist, *Nature* **279**, 651 (1979).
14 M. Buckle and H. Buc, *Biochemistry* **28**, 4388 (1989).
15. K. Kirkegaard, H. Buc, A. Spassky, J. C. Wang, *Proc. Natl. Acad. Sci. U.S.A.* **80**, 2544 (1983).
16. P. Schickor, W. Metzger, W. Werel, H. Lederer, H. Heumann, *EMBO J.* **9**, 2215 (1990).
17. The intrinsic $KMnO_4$ reactivities of T and C appear to be essentially independent of temperature over the range examined. Small differences, if any, could not be quantified because no internal control band was present.
18. $KMnO_4$ reactivity ratios at +1T, +2T, −11T, and −12C decrease with increasing temperature on both supercoiled (Fig. 1D) and linear DNA (Fig. 2) because $KMnO_4$ reactivity at these flanking positions in RP_{o1} increases with increasing temperature. This effect may result from the transient opening of these flanking bases in RP_{o1} by thermal fluctuations or from a small extent of conversion of RP_{o1} to RP_{o2} with increasing temperature in the absence of Mg^{2+}. [The extent of any thermally induced conversion of RP_{o1} to RP_{o2} appears small because the increase in $KMnO_4$ reactivity at +1T and +2T upon addition of 10 mM Mg^{2+} (Fig. 1, A and B) is large even at 25° and 37°C.]
19. J. E. Lusk, R. J. P. William, E. P. Kennedy, *J Biol. Chem.* **243**, 2618 (1968); T. Alatossava, H. Jutte, A. Kuhn, E. Kellenberger, *J. Bacteriol.* **162**, 413 (1985).
20. M. T. Record, Jr., J.-H. Ha, M. Fisher, *Methods Enzymol.* **208**, 291 (1991).
21. C.-W. Wu and D. A. Goldthwait, *Biochemistry* **8**, 4458 (1969), R. Koren and A. S. Mildvan, *ibid.* **16**, 241 (1977).
22. C. Zwieb and S. Adhya, in *Methods in Molecular Biology*, G. G. Kneale, Ed. (Humana, Totowa, NJ, in press).
23. M. P. Kladde, J. D'Cunha, J. Gorski, *J. Mol. Biol.*, in press.
24. F. Sanger, S. Niklen, A. R. Coulson, *Proc. Natl. Acad. Sci. U.S.A.* **74**, 5463 (1977).
25. We gratefully acknowledge the many significant contributions of R. Gourse and C. A. Gross to this work. We also thank P. Richey, P. Schlax, D. Frank, and M. P. Kladde for discussions and comments on the manuscript, the referees for constructive criticisms, and S. Aiello for assistance in its preparation. Supported by NIH grants GM23467 and GM37048.

14 August 1992; accepted 13 November 1992

Molecular Mapping and Detoxification of the Lipid A Binding Site by Synthetic Peptides

Alessandro Rustici, Massimo Velucchi, Raffaella Faggioni, Marina Sironi, Pietro Ghezzi, Sally Quataert, Bruce Green, Massimo Porro*

Endotoxin [lipopolysaccharide (LPS)], the major antigen of the outer membrane of Gram-negative bacteria, consists of a variable-size carbohydrate chain that is covalently linked to *N,O*-acylated β-1,6-D-glucosamine disaccharide 1,4′-bisphosphate (lipid A). The toxic activity of LPS resides in the lipid A structure. The structural features of synthetic peptides that bind to lipid A with high affinity, detoxify LPS in vitro, and prevent LPS-induced cytokine release and lethality in vivo were defined. The binding thermodynamics were comparable to that of an antigen-antibody reaction. Such synthetic peptides may provide a strategy for prophylaxis and treatment of LPS-mediated diseases.

Bacterial LPS produces a plethora of biological effects in mammals via its lipid A moiety, which is the conserved hydrophobic region (*1*). The toxic activity of LPS is related to the induction of tumor necrosis factor (TNF) release after LPS binds to macrophages and monocytes, with the consequent activation of the cytokine cascade that involves interleukin-1 (IL-1) and IL-6 (*2, 3*). Mortality from endotoxicosis consequent to sepsis is 20 to 60% (*4*). LPS has also been proposed as a potent activator of human immunodeficiency virus type 1 (HIV-1) expression in monocytes and macrophages (*5*) and as the agent that produces the symptoms characteristic of acute graft-versus-host disease (GVHD) (*6*).

Polymyxin B (PmB), a cationic cyclic peptide antibiotic, inhibits the biological effects of LPS through its high-affinity binding to lipid A (*7*). The effects that are inhibited by PmB include the Shwartzman reaction (*8*), B-II cell mitogenicity (*9*), TNF and IL-1 release from macrophages and monocytes (*10, 11*), anticomplementary activity (*12*), pyrogenic reaction in rabbits (*13*), and lethality in mice (*8, 14*). The structural features of PmB that permit binding to and detoxification of lipid A are unknown, and its use for treatment of septic shock (*10*) is limited by its high toxicity (*8, 14*). Accordingly, we have designed synthetic peptides (comprised of L-amino ac-

A. Rustici, M. Velucchi, M. Porro, Biosynth Research Laboratories, Rapolano Terme, Siena, Italy 53040.
R. Faggioni, M. Sironi, P. Ghezzi, Istituto di Ricerche Farmacologiche "Mario Negri," Milan, Italy 20157.
S. Quataert and B. Green, Lederle-Praxis Biologicals, Rochester, NY 14623.
*To whom correspondence should be addressed.

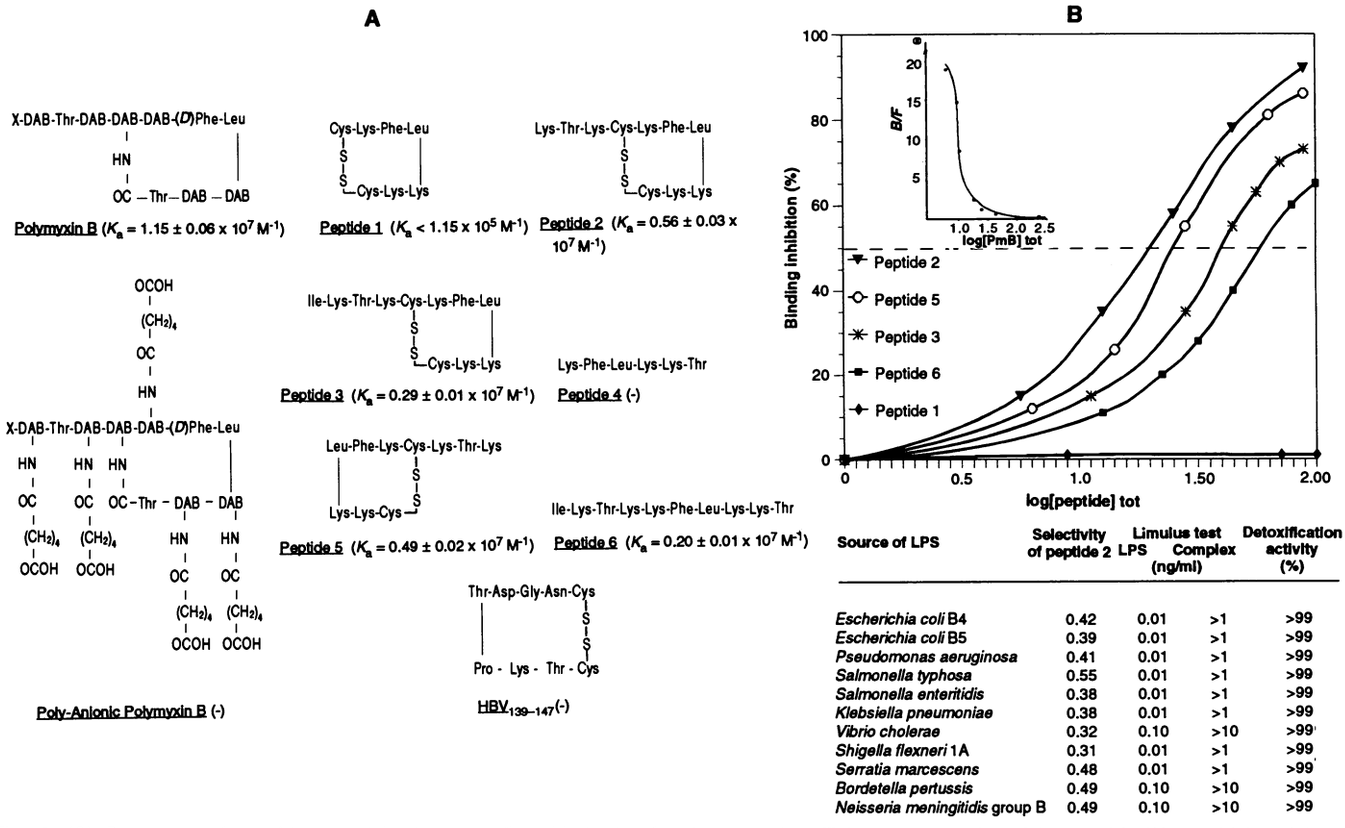

Source of LPS	Selectivity of peptide 2	Limulus test LPS	Limulus test Complex (ng/ml)	Detoxification activity (%)
Escherichia coli B4	0.42	0.01	>1	>99
Escherichia coli B5	0.39	0.01	>1	>99
Pseudomonas aeruginosa	0.41	0.01	>1	>99
Salmonella typhosa	0.55	0.01	>1	>99
Salmonella enteritidis	0.38	0.01	>1	>99
Klebsiella pneumoniae	0.38	0.01	>1	>99
Vibrio cholerae	0.32	0.10	>10	>99
Shigella flexneri 1A	0.31	0.01	>1	>99
Serratia marcescens	0.48	0.01	>1	>99
Bordetella pertussis	0.49	0.10	>10	>99
Neisseria meningitidis group B	0.49	0.10	>10	>99

Fig. 1. (**A**) Structures of peptides used in these studies. Methods of synthesis and analysis are described in (*15*). We calculated binding affinities (K_a) for *B. pertussis* LPS and *B. pertussis* lipid A measuring selectivity (B) with respect to the affinity of PmB. We calculated the affinity of PmB for *B. pertussis* LPS and *B. pertussis* lipid A at the midpoint of the binding curve by plotting the value of PmB bound/free (B/F) versus the total amount of PmB in reaction (PmB tot) (*31*) (B). The concentrations of PmB (μM) were measured by high-performance liquid chromatography (HPLC) analysis at a wavelength of 220 nm. DAB, α-γ-diaminobutyric acid; X, 6-methyl heptanoyl/octanoyl. $HBV_{139-147}$, hepatitis B virus S-gene amino acid sequence 139 to 147 (*16*). (**B**) Selectivity of binding of synthetic peptides for the lipid A binding site of *B. pertussis* LPS and for LPS of different Gram-negative bacteria. Each inhibition curve was estimated by direct competition of the peptides with PmB for *B. pertussis* lipid A and LPS in either water or phosphate-buffered saline (PBS) at 37°C. The concentration of peptide displacing 50% of PmB from lipid A or LPS complexes determines the value of selectivity and expresses the ratio between the affinity constant value of the peptide (K_a peptide) and that of PmB (K_a PmB). PmB was used in the competition analysis at a concentration corresponding to the maximum precipitating activity, in water, for LPS (6.3 μM PmB precipitated 6.0 μM of *B. pertussis* lipid A or LPS). The concentrations of PmB and peptide competitors (μM) were measured by reversed-phase HPLC (Waters-Millipore, Milford, Massachusetts) analysis at a wavelength of 220 nm, with a linear methanol in water gradient of 20 to 80%. The calculated selectivities for the peptides were as follows: peptide 2, 0.49; peptide 5, 0.43; peptide 3, 0.25; peptide 6, 0.17; and peptide 1, <0.01. Detoxification activity of peptide 2 in limulus test (see Table 1 for definition and conditions) for different LPSs was tested with the complexes formed at 1:1 (w/w) peptide:LPS ratio. The lowest concentration of LPS, free or in complex, giving a positive assay (clotting) is reported. LPSs from *B. pertussis* and *Neisseria meningitidis* were purified according to the method described in (*32*). All other LPSs were commercially available (Sigma). Lipid A was purified according to the method described in (*33*).

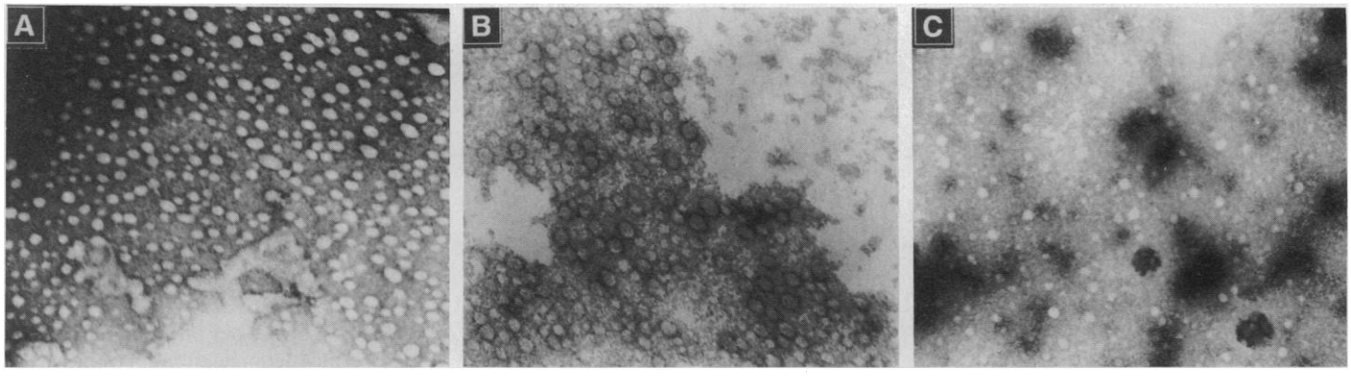

Fig. 2. Electron micrographs (original magnification, ×130,000) of *B. pertussis* lipid A (**A**) and LPS (**B**) micelles in complex with the synthetic cyclic peptide 2. Micelles of purified LPS are shown in (**C**). Peptide molecules are shown as a dark area surrounding the micelles. Electron microscopy was performed with negative staining [1% (w/v) uranyl acetate]. Samples were mounted at a concentration of 100 μg/ml in PBS [(A) and (B)] or in 0.1 M sodium citrate (C). One centimeter corresponds to 104 nm.

Table 1. Characteristics of synthetic peptides (*15*).

Peptide	Limulus test*	Antibiotic activity (mg/ml)†	Hemolytic activity (mg/ml)‡	Half-life (min) in whole blood§	Pyrogenicity of peptide-LPS complex (Δ°C)‖		% Lethality¶
					2 hours	3 hours	
Polymyxin B	Negative (1)	0.008	>1.50	>180 (100)	−0.19	−0.38	100 (10)
Peptide 1	Negative (10)	>1.00	>1.50	>180 (70)	−0.51	−0.33	0 (60)
Peptide 2	Negative (1)	>1.00	>1.50	50 (10)	−0.28	−0.30	0 (60)
Peptide 3	Negative (2)	>1.00	>1.50	>180 (76)	ND	ND	0 (60)
Peptide 4	Positive (1000)	ND	>1.50	ND	ND	ND	ND
Peptide 5	Negative (1)	ND	>1.50	18 (−)	ND	ND	ND
Peptide 6	Negative (2)	ND	>1.50	50 (28)	ND	ND	ND
Polyanionic Polymyxin B	Positive (100)	ND	ND	ND	+0.62	+0.71	ND
HBV 139-147 (*16*)	Positive (100)	ND	ND	ND	+0.53	+0.94	ND

*Limulus amoebocyte lysate test (sensitivity 0.125 EU/ml) was done according to the manufacturer's instructions (Whittaker, Walkersville, Maryland) with LPS purified from *B. pertussis*. The minimal peptide:LPS ratio (w/w) that inhibited clot formation after preincubation for 15 min at 37°C (negative test) is listed in parentheses. †Antibiotic activity of the peptides (milligrams per milliter on filter disk) was estimated by determination of the minimal inhibiting concentration on plates of beef-heart infusion medium, inoculated with a liquid culture of *Salmonella typhimurium, Haemophilus influenzae*, and *Vibrio cholerae*. The zone inhibition was read after 18 hours. ‡Hemolytic activity of the peptides was estimated after equal volumes of the peptides were incubated with 10% fresh human red blood cells in saline for 30 min at 37°C. §Stability of the peptides to trypsin-like enzymes was investigated by incubation of the peptides (2.5 mg/ml) with human serum or whole blood ex vivo at 37°C for 180 min. Portions were removed at $t = 0$ and at 30-min intervals and processed by reversed-phase HPLC analysis to quantitate the amount of residual peptide. The half-life of the peptides and the percentage recovered after 180-min hydrolysis (given in parentheses) was calculated for PmB and the peptides. Enzymatic activity of the serum was titered by the synthetic peptide substrate Val-Ser-Arg-*p*-nitroanilide at a wavelength of 410 nm. ‖Pyrogenicity of peptide-LPS complexes in rabbit was determined according to the pyrogen test (*34*). The pyrogenic activity of purified *B. pertussis* LPS injected intravenously (30 ng per kilogram of body weight; mean of the temperature increase: 2 hours, +0.55°C; and 3 hours, +0.90°C) was compared to preformed complexes at the following w/w ratios: PmB or peptide 2: LPS = 2, peptide 1: LPS = 10; hepatitis B virus S-gene amino acid sequence 139–147 ($HBV_{139-147}$) or polyanionic PmB:LPS = 100. Data express the mean of the temperature rise from the basal temperature. ¶Acute toxicity and lethality in mice (strain CD1 and BALB/c) was tested in groups of ten mice for each component. PmB and peptides [dose (milligrams per kilogram of body weight) given in parentheses] were injected intravenously according to the procedure reported for General Drug Safety Test of the U.S. Pharmacopeia (*34*). Animals were observed for 48 hours and beyond. ND, not done.

ids) that mimic the primary and secondary structure of PmB in order to determine the minimal and optimal features required for binding to and detoxification of lipid A.

Various peptides were synthesized; the secondary rearrangement (conformation) of some peptide structures was attained by cyclization via an intramolecular disulfide bridge resulting from oxidation of two cysteine residues inserted in the primary amino acid structure (Fig. 1A).

Peptide conformation (linear versus cyclic) affected the relative values of affinity (selectivity) for binding to lipid A and LPS, as detected by competition studies (Fig. 1B). Peptide 4, a linear peptide that mimics the primary amino acid sequence of the PmB cyclic conformation, does not exhibit binding activity, as compared to the same amino acid sequence in a cyclic conformation (peptide 1). However, peptide 1, in contrast to peptide 2, does not compete with PmB significantly, an indication that even the size of the peptide is a factor affecting optimal filling of the binding site. Likewise, the affinity of the linear peptide 6, which mimicked the primary amino acid sequence of PmB, was less than that of the same sequence rearranged in a cyclic conformation (peptide 3). In contrast, retro-orientation of peptide 2 (the retroisomer peptide 5) did not significantly affect the affinity; thus, specific orientation of the peptide bonds is not required for binding. In all cases, the complexes of lipid A with the synthetic peptides had a stoichiometry (*15*) comparable to that of the complex formed with PmB (*7*), and binding followed by detoxification occurred with the lipid A of different LPSs (Fig. 1B). Finally, neither a non-PmB–related cyclic peptide (*16*) nor the anionic derivative of PmB could bind (Fig. 1A) and detoxify lipid A (Table 1).

Our data indicate that multiple factors are responsible for optimal binding of peptide structures to lipid A, including the

Table 2. Inhibition of LPS-induced TNF and IL-6 release in the serum of mice after treatment with LPS from *E. coli* 055:B5. Data express the mean of serum TNF and IL-6 concentrations measured 60 and 120 min, respectively, after treatment with LPS, in two groups of five mice each (strain CD1, Charles River). TNF was measured by a standard cytotoxicity assay, with L929 cells (*35*) and recombinant human TNF as a standard. IL-6 bioactivity was measured as hybridoma growth factor activity on 7TD1 cells, with recombinant human IL-6 as a standard (*36*). Peptides were injected intravenously at a dose of 100 μg, 30 min before intraperitoneal LPS administration (0.1 μg/mouse). Statistical significance was calculated by the *t* test.

Compound	Serum TNF (ng/ml) ± SE	Percent inhibition (significance)	Serum IL-6 (ng/ml) ± SE	Percent inhibition (significance)
Saline	18.07 ± 4.95		4.84 ± 1.35	
Peptide 1	3.09 ± 1.08	83 ($P < 0.01$)	1.31 ± 0.41	73 ($P < 0.05$)
Peptide 2	1.25 ± 0.82	93 ($P < 0.001$)	0.78 ± 0.37	84 ($P < 0.05$)
Peptide 3	3.25 ± 1.62	82 ($P < 0.01$)	1.23 ± 0.72	75 ($P < 0.05$)
PmB	1.45 ± 0.72	92 ($P < 0.001$)	0.46 ± 0.19	90 ($P < 0.05$)

Table 3. Survival rate in mice. Strain CD1 mice treated with low-dose LPS from *E. coli* 055:B5 were injected intravenously with peptide 2 (0.25 mg per mouse) and PmB (0.1 mg per mouse, highest dose tolerated) and then injected intraperitoneally with actinomycin-D (30 μg per mouse) and LPS (2.5 μg per mouse) 30 min later. BALB/c mice were treated with high-dose LPS from *E. coli* 055:B5. Mice were injected intravenously with peptide 2 or 3 (1.1 mg per mouse) and PmB (0.1 mg per mouse, highest dose tolerated) 30 min after intraperitoneal injection with LPS (1.1 mg per mouse). Data are from groups of 20 mice for each experiment. Survival was followed daily for 7 days. The number of surviving mice (as a percentage of the total) is given in parentheses. Statistical significance was calculated by Fisher's exact test, 7 days after LPS treatment.

Compound	Surviving mice at				Significance
	24	48	72	168 hours	
	Post-treatment with low-dose LPS				
Saline	5 (25)	3 (15)	1 (5)	1 (5)	
Peptide 2	13 (65)	8 (40)	8 (40)	8 (40)	$P < 0.01$
PmB	10 (50)	8 (40)	6 (30)	6 (30)	$P < 0.05$
	Pre-treatment with high-dose LPS				
Saline	10 (50)	6 (30)	6 (30)	6 (30)	
Peptide 2 or 3	20 (100)	12 (60)	12 (60)	8 (40)	$P > 0.05$
PmB	12 (60)	8 (40)	8 (40)	8 (40)	$P > 0.05$

amphipathic and cationic features of the primary amino acid sequence, the size of the structure, and the peptide conformation. However, addition of the alkyl chain of L-isoleucine to peptide 2 (peptide 3) negatively affected the binding affinity. This contrasts with the speculated hydrophobic interactions of PmB with lipid A through its 6-methyl-octanoyl/heptanoyl chain (*7*). Because binding of the peptides to lipid A was not affected by pH (range 2 to 11) or ionic strength (range 0.01 to 0.5 M), the hydrophobic binding probably involves the Phe-Leu present in the cyclic, conformationally stable peptide structure. The alkyl chain of the lysine residues may also contribute to binding efficiency; however, their cationic (at physiologic pH) amino groups, although likely interacting with the phosphate groups of lipid A, do not seem to play a major role in the binding because all the ε-amino groups of the lysine residues of peptide 2 were still completely reactive to the picrylsulfonic acid reagent (*17*) when in complex with lipid A (*18*).

Electron microscopy of the precipitated peptide–lipid A or peptide-LPS complexes provided evidence that micelle aggregates of lipid A or LPS were surrounded by a dark halo of peptide molecules (Fig. 2). On the basis of the measured 1:1 peptide:lipid A stoichiometry, we used computer-assisted modeling (*19*) to compare the dimensions of the most affine peptide with those of lipid A as *N,O*-acylated β-1,6-D-glucosamine disaccharide 1,4′-bisphosphate monomer (*20*). The calculated dimensions of peptide 2 (25.6 by 14.0 by 10.7 Å) and those of the hydrophobic pocket formed by the *N,O*-acyl residues of the lipid A monomer (23.5 by 23.9 by 20.9 Å) are similar to the combining site of an antibody that binds to a trisaccharide epitope (*21*). Peptides of appropriate sequence and structure do bind to lipid A with a saturation curve (Fig. 1B) comparable to that of the epitope-specific homogeneous population of antibodies that are induced by bacterial oligosaccharide haptens conjugated to carrier protein (*22, 23*).

We compared binding affinity and functional activity of the peptides by assaying inhibition of LPS-induced clot formation in the limulus amoebocyte lysate (LAL) assay (Table 1). Higher affinity peptides were more potent inhibitors of the enzymatic reaction. Efficacy of LPS detoxification by synthetic peptides was tested in vivo with LPSs of *Bordetella pertussis* and *Escherichia coli*, which have different activities (Fig. 1B) and lipid A structures, with five and six *N,O*-acyl chains of different length, respectively (*24, 25*). Detoxification of *B. pertussis* LPS was monitored by the febrile response of rabbits, and that of *E. coli* LPS was monitored by the cytokine release in mice. The febrile response to LPS involves two distinct temperature increases: the first increase is shown within 2 hours of the injection of LPS, whereas the second (and more consistent) increase appears in the third hour and is mediated by TNF and IL-1 (*13, 26*). The LPS-peptide complexes did not show either of the temperature increases (Table 1), which demonstrates the stability of the complexes in vivo and suggests that the release of the two endogenous pyrogens (TNF and IL-1) was inhibited after reaction with the peptides. TNF release was significantly inhibited in mice when the peptides were injected either in complex or before treatment with *E. coli* LPS. IL-6 production was also significantly inhibited (Table 2), and LPS toxicity was reduced, as shown by a significant increase in the survival rate (Table 3). When the peptides were injected after LPS treatment, complete protection was observed at 24 hours, but lethality was only delayed (Table 3), in agreement with data indicating that triggering of TNF production occurs in vivo within a few minutes of LPS injection (*27*). However, the doses of LPS that produced significant lethality in mice were much higher than the maximum serum concentrations (0.1 ng/ml) found in septic patients (*28*).

In contrast to PmB, our peptides have shown neither antibiotic activity nor acute toxicity and lethality when injected intravenously into mice at a dose as high as 60 mg per kilogram of body weight (Table 1). PmB is lethal in mice at a dose of 5 mg/kg (*14*), and at 10 mg/kg caused 100% lethality in BALB/c and CD1 mice. Safety of the synthesized peptides was anticipated on the basis of their L-amino acid composition and their degradation characteristics, which contrast with those of PmB, which is refractory to biological degradation by serine proteases in human serum (Table 1). Also, unlike natural cationic and amphipathic peptide antibiotics such as melittins, which have strong hemolytic activity on red blood cells (*29*), the reported peptides have no lytic activity on human erythrocytes (Table 1).

Elucidation of the lipid A binding site by peptide structures may enhance our understanding of the nature of mammalian receptor proteins for LPS and suggests a strategy for the design of anti-LPS molecules as drugs and peptide–lipid A complex–based vaccines that may be useful in the prophylaxis and treatment of LPS-mediated diseases.

REFERENCES AND NOTES

1. C. R. H. Raetz, *Annu. Rev. Biochem.* **59**, 129 (1990).
2. H. Loppnow *et al.*, *Infect. Immun.* **58**, 3743 (1990).
3. C. A. Dinarello, *J. Infect. Dis.* **163**, 1177 (1991).
4. E. J. Ziegler *et al.*, *N. Engl. J. Med.* **324**, 429 (1991).
5. R. G. Pomerantz, M. B. Feinberg, D. Trono, D. Baltimore, *J. Exp. Med.* **172**, 253 (1990).
6. F. P. Nestel, K. S. Price, T. A. Seemayer, W. S. Lapp, *ibid.* **175**, 405 (1992).
7. D. C. Morrison and D. M. Jacobs, *Immunochemistry* **13**, 813 (1976).
8. W. A. Craig, J. H. Turner, C. M. Kunin, *Infect. Immun.* **10**, 287 (1974).
9. G. T. Spear and M. Teodorescu, *J. Immunol. Methods* **73**, 321 (1984).
10. D. C. Stokes *et al.*, *J. Infect. Dis.* **160**, 52 (1989).
11. J. Cavaillon and N. Haeffner-Cavaillon, *Mol. Immunol.* **23**, 965 (1986).
12. T. Yockochi, Y. Inoue, Y. Kimura, N. Kato, *J.*

Immunol. **144**, 3106 (1990).
13. T. Shimozato, M. Iwata, N. Tamura, *Infect. Immun.* **58**, 1384 (1990).
14. D. Rifkind, *J. Bacteriol.* **93**, 1463 (1967).
15. Peptides were synthesized on solid phase with 9-fluorenyl methyloxycarbonyl amino acid derivatives (*30*) (Milligen, Burlington, MA) in an automatic Milligen 9050 peptide synthesizer. Peptides were cleaved (2 hours at room temperature) from the resin support by 95% trifluoroacetic acid, with 5% ethane dithiol as scavenger, when peptides contained cysteine residues as cysteine-*S*-trityl derivatives. Peptides (0.1 mg/ml, pH 7.0) were cyclized by air oxidation with vigorous stirring for 2 to 24 hours, conditions under which only intrachain disulfide bridges form (cyclic monomers), as verified by their masses [determined by fast atom bombardment (FAB) mass spectrometry]. Peptides were purified by reversed-phase HPLC with a linear methanol in water gradient of 20 to 80%. Amino acid composition of the peptides was confirmed by Pico-Tag analysis (Waters). Quantitation of amino groups in the peptides was as described (*17*). Oxidation of the thiol groups of cysteine residues was ascertained by Ellman's reagent. Purity was confirmed by measurement of the mass of each peptide by FAB mass spectrometry with the use of a VG 70-250 S spectrometer. Polyanionic PmB was prepared by reaction of PmB with a fivefold molar excess of bis-succinimidyl ester of adipic acid (*22*). Amino groups of PmB were converted to carboxyl groups after mild hydrolysis of the resulting monosuccinimidyl ester derivatives by 10^{-3} M sodium hydroxide for 1 hour at room temperature. Stoichiometry of peptide–lipid A and LPS complexes (1:1 mol/mol) of LPS from *B. pertussis*, *S. typhosa*, and *E. coli* 055:B5 was detected by amino acid and D-glucosamine content of the precipitated complexes by Pico-Tag analysis.
16. S. E. Brown, C. R. Howard, A. J. Zuckerman, M. W. Steward, *J. Immunol. Methods* **72**, 41 (1984).
17. A. F. S. A. Habeeb, *Anal. Biochem.* **14**, 328 (1966).
18. Lipopolysaccharide (0.7 mg) from *S. typhosa* was complexed by 0.1 mg of peptide 2 (1:1 mol/mol peptide:lipid A) in water. The complex was then solubilized in 4% sodium bicarbonate and reacted with 0.1% picrylsulfonic acid (*17*) for 2 hours at 37°C. Six moles of amino groups per mole of peptide were detected in the complex. The sample was further processed by gel chromatography on agarose A1.5m (Bio-Rad, Richmond, CA). The picrylsulfonic acid–derived peptide coeluted with LPS at the void volume (molecular weight exclusion >1.5 million) of the column, as detected by amino acid analysis (Pico-Tag method) of the eluates.
19. Space-filling models of peptide 2 and the monomer unit of *B. pertussis* lipid A (*20*) were produced with Alchemy II software (Tripos Associates Inc, St. Louis, MO) on an HP-Vectra 486/33T 33 MHz computer and were elaborated in condition of minimal energy with cut-off 0.01.
20. M. Caroff and L. Szabo, *Carbohydr. Res.* **114**, 95 (1983).
21. M. Cygler, D. R. Rose, D. R. Bundle, *Science* **253**, 442 (1991).
22. M. Porro *et al.*, *Mol. Immunol.* **22**, 907 (1985); *ibid.* **23**, 385 (1986).
23. B. Arndt and M. Porro, in *Immunobiology of Proteins and Peptides*, M. Z. Atassi, Ed. (Plenum, New York, 1991), vol. 6, pp. 129–148.
24. M. Caroff, J. M. Cavaillon, C. Fitting, N. Haeffner-Cavaillon, *Infect. Immun.* **54**, 465 (1986).
25. S. Kotani *et al.*, *ibid.* **49**, 225 (1985).
26. C. A. Dinarello, *Agents Actions* **13**, 470 (1983).
27. T. R. Ulich, K. Guo, J. Del Castillo, *Am. J Pathol.* **134**, 11 (1989).
28. S. D. Wright, *Science* **252**, 1321 (1991).
29. D. Wade *et al.*, *Proc. Natl. Acad. Sci. U.S.A.* **87**, 4761 (1990).
30. E. Atherton, C. J. Logan, R. C. Sheppard, *J. Chem. Soc. Perkin Trans.* **1**, 538 (1981).
31. J. A. Berzofsky, *Clin. Chem.* **24**, 419 (1978).
32. O. Westphal, O. Luderitz, F. Bister, *Naturforscher.* **7**, 148 (1952).
33. M. Caroff, A. Taken, L. Szabo, *Carbohydr. Res.* **175**, 273 (1988).
34. *U.S. Pharmacopeia, vol. XXI/The National Formulary, vol. XVI*, combined edition, the United States Pharmacopeial Convention, Rockville, MD, 1985.
35. B. B. Aggarwal *et al.*, *J. Biol. Chem.* **260**, 2345 (1985).
36. M. F. Sironi *et al.*, *J. Immunol.* **142**, 549 (1989).

37. We thank Maria Pia Brachini for typing the manuscript; Cecilia Leonardi, Antonella Martinuzzi, and Marcello Porro for laboratory support; and Dr. G. Giorgi, Laboratory of Structural Analysis, University of Siena, for FAB-MASS spectrometry.

13 July 1992; accepted 13 October 1992

Sequence-Specific Binding of Transfer RNA by Glyceraldehyde-3-Phosphate Dehydrogenase

Ravinder Singh and Michael R. Green

A transfer RNA (tRNA) binding protein present in HeLa cell nuclear extracts was purified and identified as the glycolytic enzyme glyceraldehyde-3-phosphate dehydrogenase (GAPDH). Studies with mutant tRNAs indicated that GAPDH recognizes both sequence and structural features in the RNA. GAPDH discriminated between wild-type tRNA and two tRNA mutants that are defective in nuclear export, which suggests that the protein may participate in RNA export. The cofactor nicotinamide adenine dinucleotide disrupted complex formation between tRNA and GAPDH and thus may share a common binding site with the RNA. Indirect immunofluorescence experiments showed that GAPDH is present in the nucleus as well as in the cytoplasm.

The primary transcripts of eukaryotic genes are processed extensively in the nucleus, and the mature RNAs are exported to the cytoplasm. Although nuclear RNA export is fundamental to gene expression, we know relatively little about its underlying mechanisms. By analogy with nuclear protein import (*1*), the process is likely to involve nuclear proteins that bind specifically to the RNAs being exported. Consistent with this prediction, nuclear export of tRNAs as well as m^7G-capped RNAs is a saturable, carrier-mediated process (*2*, *3*). Furthermore, specific mutations within tRNA (*4*) and 5S ribosomal RNA (*5*) can block export of these RNAs.

The single base substitution G57U in human $tRNA_i^{Met}$ has been shown to reduce nuclear export of the RNA in microinjected frog oocytes (*4*). To identify proteins that participate in tRNA export, we looked for nuclear proteins that bound to wild-type $tRNA_i^{Met}$ but not to the G57U mutant. As measured by an RNA mobility-shift assay, we found such an activity in the 0.1 M KCl DEAE-Sepharose fraction of a HeLa cell nuclear extract (*6*). This tRNA binding activity was further fractionated, and the polypeptide composition of the chromatographic fractions was monitored by SDS–polyacrylamide gel electrophoresis (Fig. 1A). The most purified fraction, the 0.5 M KCl eluate from the polyuridylic acid [poly(U)] column, contained a single polypeptide of approximately 37 kD. Both the partially purified (*6*) and the homogeneous preparations of the 37-kD protein discriminated between the wild-type $tRNA_i^{Met}$ and the G57U mutant (Fig. 1B). The tRNA binding activity was heat-labile and resistant to digestion with micrococcal nuclease (*6*). The 37-kD polypeptide was then purified in sufficient quantity for microsequence analysis. A tryptic peptide derived from the protein was found to contain the sequence LISWYDNEFGYSNR (*7*). A database search revealed that this peptide sequence is present within the COOH-terminal region of glyceraldehyde-3-phosphate dehydrogenase (GAPDH), a 37-kD glycolytic enzyme (*8*).

To determine whether tRNA binding was mediated by GAPDH, we performed an immunodepletion experiment. A binding reaction mixture containing ^{32}P-labeled tRNA and the purified 37-kD protein was incubated with either a polyclonal antibody to GAPDH or preimmune serum, and the resulting antigen-antibody complexes were removed with Pansorbin (Calbiochem, San Diego, California). The antibody to GAPDH, but not the preimmune serum, depleted the tRNA-protein complex from the supernatant (*6*).

A commercial preparation of human GAPDH (Sigma) also contained tRNA binding activity, and, like the 37-kD protein, bound to wild-type $tRNA_i^{Met}$ but not to the G57U mutant (Fig. 1B). Neither the 37-kD protein nor the commercial GAPDH bound to VA1 RNA, an unrelated adenoviral RNA transcribed by RNA polymerase III. Taken together (*9*), these data provide strong evidence that the tRNA binding activity was in fact GAPDH.

GAPDH also bound to in vitro–transcribed *Escherichia coli* $tRNA^{Tyr}$ and yeast

Program in Molecular Medicine, University of Massachusetts Medical Center, Worcester, MA 01605.